INL/CON-14-31745
PREPRINT

Developing a Laser Shockwave Model for Characterizing Diffusion Bonded Interfaces

41st Annual Review of Progress in Quantitative Nondestructive Evaluation

Jeffrey M. Lacy, James A. Smith and Barry H. Rabin

July 2014

The INL is a
U.S. Department of Energy
National Laboratory
operated by
Battelle Energy Alliance

Developing a Laser Shockwave Model for Characterizing Diffusion Bonded Interfaces

Jeffrey M. Lacy[1 a)], James A. Smith[1], Barry H. Rabin[1]

[1]*Idaho National Laboratory, Idaho Falls ID*
[a)]*Jeffrey.Lacy@inl.gov*

Abstract. The US National Nuclear Security Agency has a Global Threat Reduction Initiative (GTRI) with the goal of reducing the worldwide use of high-enriched uranium (HEU). A salient component of that initiative is the conversion of research reactors from HEU to low enriched uranium (LEU) fuels. An innovative fuel is being developed to replace HEU in high-power research reactors. The new LEU fuel is a monolithic fuel made from a U-Mo alloy foil encapsulated in Al-6061 cladding. In order to support the fuel qualification process, the Laser Shockwave Technique (LST) is being developed to characterize the clad-clad and fuel-clad interface strengths in fresh and irradiated fuel plates. LST is a non-contact method that uses lasers for the generation and detection of large amplitude acoustic waves to characterize interfaces in nuclear fuel plates. However, because the deposition of laser energy into the containment layer on a specimen's surface is intractably complex, the shock wave energy is inferred from the surface velocity measured on the backside of the fuel plate and the depth of the impression left on the surface by the high pressure plasma pulse created by the shock laser. To help quantify the stresses generated at the interfaces, a finite element method (FEM) model is being utilized. This paper will report on initial efforts to develop and validate the model by comparing numerical and experimental results for back surface velocities and front surface depressions in a single aluminum plate representative of the fuel cladding.

INTRODUCTION

The U.S. National Nuclear Security Agency supports the Global Threat Reduction Initiative with the goal of reducing the use of highly enriched uranium (HEU) worldwide. A part of that initiative is the conversion of research reactors from HEU to low-enriched uranium (LEU) fuels. The U.S. High Performance Research Reactors program is testing and qualifying a new high-uranium density fuel to supplant the HEU dispersion fuels used in some high performance reactors [1]. The LEU fuel will be based on a fuel meat made from a monolithic uranium-10 wt.% molybdenum (U–10Mo) alloy foil (typically 0.2 to 0.4 mm thick) encapsulated in 6061 aluminum cladding using a hot isostatic press (HIP) process, with thin (typically 25 μm) Zr diffusion barrier interlayers between the U–10Mo and cladding, as shown schematically in Fig. 1.

One major difference between monolithic fuel and typical dispersion fuels relates to the fuel-cladding interfaces. In monolithic fuel, a difference in properties exists across the fuel cladding interface, creating localized stresses during fabrication and irradiation. Furthermore, the interface comprises complex microstructures that change over time. Characterizing the condition of the fuel in both the as-fabricated (fresh) and irradiated state is imperative for validating safe reactor operations and evaluating fuel performance. Specifications exist to ensure that mechanical reliability and temperature of the fuel are maintained as well as to ensure that fuel-cladding bonding is adequate. Because the cladding functions as the principal barrier for fission product retention, further requirements pertaining to safeguarding cladding-cladding bonding during normal operating conditions are imposed. Characterization of bond strength in fuel plates using typical mechanical testing techniques is difficult. Therefore, a need exists to implement new assessment methods and measures for evaluating interface bonds within fuel plates suitable for both fresh and irradiated fuels.

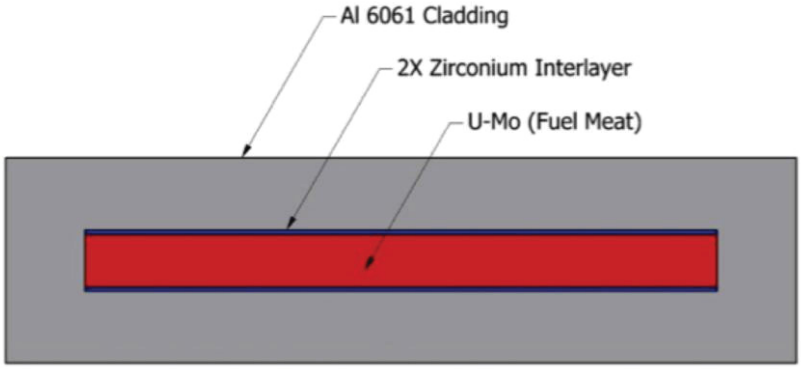

FIGURE 1. Schematic cross-section of a monolithic fuel plate

Background

In the Laser Shockwave Technique (LST), initially developed for determining adhesion of thin films and coatings to substrates [2-7], a high-energy pulsed laser generates a compressive shock wave at the upper surface of a test sample. The compressive shock traverses the specimen. After arriving at the bottom of the test sample, the compressive wave is transformed by the free surface into a tensile wave that traverses back through the specimen. A shock wave with amplitude above a threshold will generate tensile stresses that can debond the film/coating from the substrate. By examining the specimen response and using shock wave propagation models, the stress necessary to debond the film/coating from the substrate can be determined. The LST method was later modified to characterize the bond strength between multiple layers in thicker structures such as epoxy bonded carbon-carbon composites [8]. This approach forms the basis for the methods discussed herein. Benefits presented by LST include the capability to provide a confined spatial measurement without disturbing the surface of the specimen with minimal surface preparation. Because there is no spread of the induced debond stresses beyond the shocked area, the test sample remains intact. This is an advantage over traditional testing methods (e.g. pull testing, bend testing or double cantilever beam methods). The non-contact and localized nature of the LST are significant benefits for characterization of radioactive materials. As an example, fuel plates can be tested remotely while keeping fuel contained within the cladding. This improves operator safety and avoids spreading radioactive contamination.

The LST is a high strain-rate characterization technique, which relies upon the propagation of waves that generate high frequency-content loads at the interfaces. The constitutive performance of a material under shock load testing is substantially different when benchmarked against quasi-static (i.e. low strain-rate) testing techniques. The main differences between the techniques stems from flow stresses in metals that are significantly elevated and deformation mechanisms that are different. Thus, the threshold stress sufficient to generate a debond (i.e. the bond strength) as determined by LST can be significantly greater than that measured by quasi-static (i.e. low strain rate) techniques such as pull testing [9,10].

Computationally, our long-term goal is to understand the structure of the traveling shocks that load the plate interfaces, and develop the capability to predict the peak interfacial tensile stress for a given plate material, geometry, and laser shock energy for a variety of fuel types. To develop confidence that such numerical results are representative of reality, the initial focus is to validate the computational approach by comparing with simplified experimental results. To this end, a simplified experiment was conducted on a homogeneous aluminum 6061-O plate (i.e. not a layered fuel plate). Laser shocks were applied to the plate at increasing energies, and the resulting surface pit size and back surface velocity time-history were recorded. Successful reproduction of the back surface velocity indicates fidelity in the stress wave intensity, duration, and structure, while pit depth and volume is indicative of material yield and work-hardening properties. The two phenomena are highly coupled—plastic deformation associated with pit formation consumes energy from the shock and strongly affects the velocity signal. Thus simultaneous agreement of both experimental measurements with model predictions is considered a strong validation of the modeling approach.

EXPERIMENTAL SETUP

A Q-Switched neodymium doped: yttrium aluminum garnet (Nd:YAG) laser, which generates optical pulses of about 10 ns with a maximum energy of 3.5 J at 1064 nm wavelength, is used to induce shock waves for interrogating the front surface of fuel plates. The energy of the laser pulse is controlled by the flash lamp delay setting. For the purposes of this paper, the shorter the flash lamp delay, the more energetic the energy pulse. However, the portion of that energy converted into the shock wave is indeterminate. During a shock experiment, the velocity of the bottom surface of the sample is recorded in real-time by an optical velocimeter based on a solid Fabry-Perot etalon and is the measure of resulting input energy. The velocimeter laser is a long pulse (>120 μs) Nd:YAG, operated at 1064 nm wavelength. Details of the etalon interferometer are provided by Arrigoni et al [11]. Laser-UT measurements are obtained from another sub-system, where generation and detection laser beams are applied on the bottom surface (i.e. pulse-echo mode), superimposed with diameter sizes of about 1 mm and 0.5 mm, respectively. During areal scanning, the step size of the scan is approximately 0.5 mm in the x and y directions on the sample surface. The UT generation laser is a Nd:YAG, operated at 532 nm wavelength with a full-width at half-maximum (FWHM) of 10 ns. The detection uses a long pulse (>120 μs) Nd:YAG laser, operated at 1064 nm wavelength and a photorefractive interferometer. The laser-ultrasonic inspection is similar to a conventional ultrasonic C-scan. Examples of the pit formed in the plate front surface and the velocity induced at the back surface are shown in Figs. 2 and 3, respectively.

To help increase the efficiency of the generated shock wave, the specimen surface is prepared with a constraining mechanism. The constraining mechanism is constructed by placing black PVC tape on the specimen surface and then placing a layer of transparent polyurethane over the PVC tape. The shock laser light travels through the clear tape. The black electrical tape absorbs the laser energy and creates a plasma. The plasma is contained by the clear tape and increases the pressure pulse time duration and amplitude. The clear tape also contains the plasma, gasses and molten materials reducing the resulting mess and provides a more hospitable environment for the delivery optics.

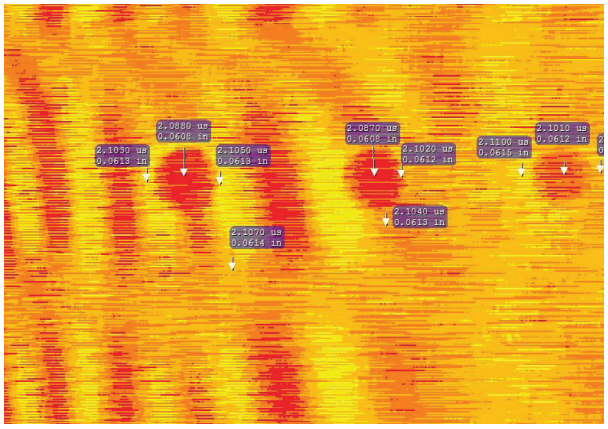

FIGURE 2. UT C-scan showing pit depth increasing with shock intensity.

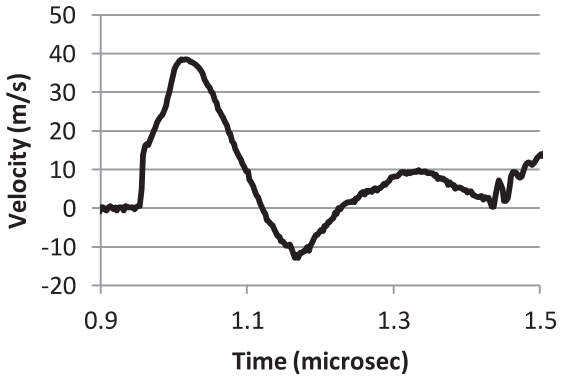

FIGURE 3. Representative measured velocity trace of plate back surface.

COMPUTATIONAL APPROACH

To pursue our objectives we employed the solid dynamics finite element code ALEGRA [12], developed and maintained by Sandia National Laboratories. ALEGRA employs an explicit integration scheme with material compressibility and a variety of strength models available, including elasticity, yield, and work hardening with rate and temperature dependence. These attributes make it ideal for our study of wave transmission, reflection, and dissipation in a multi-layered system.

All studies were conducted in an Eulerian framework, which maintains a geometrically fixed finite element mesh while allowing material to advect through it. This simplifies some aspects of the study, such as thickness parametrics, in that we do not need to generate a new mesh for each geometric instance. Figure 4 shows the model as presented in the following discussion, with a pressure pulse traveling away from the energy deposition zone at time t=100 nanosec.

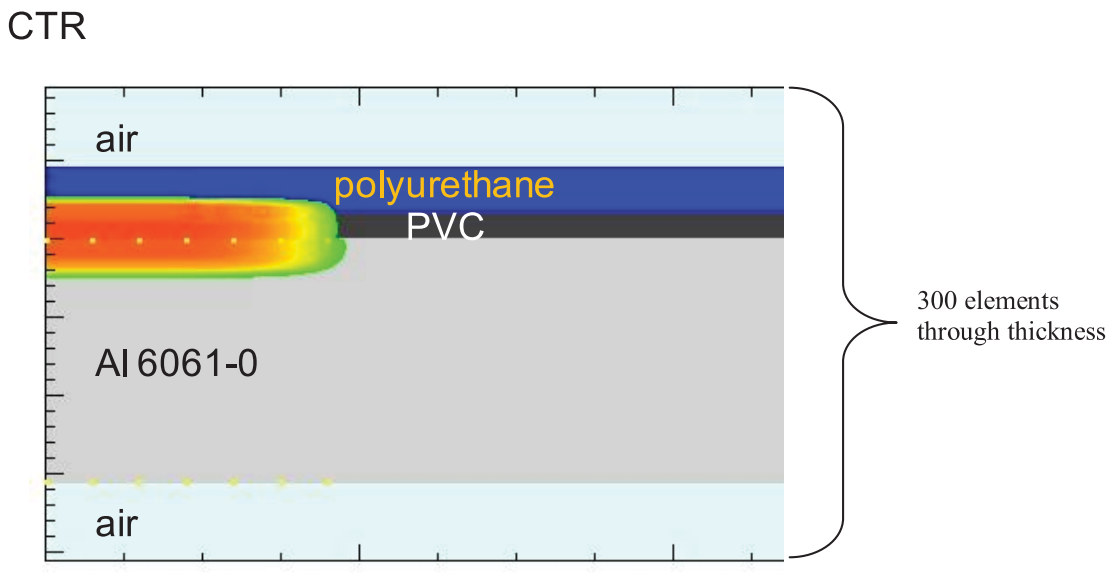

FIGURE 4. Computational domain showing material layers and pulse travelling from energy source.

Geometry

Domain development begins with the simplifying assumption that the laser is oriented perpendicular to the plate, the spot is nearly circular, and the shot location is remote from any plate edges. Then the geometry becomes cylindrical with the axis along the laser beam and the radial dimension along the plate surface. The axial size of the domain includes the thickness of the clear cover tape, black absorption tape, metallic plate, and air at ambient temperature and pressure above and below the plate. The radial dimension is selected to be the minimum necessary to avoid wave reflections from the domain boundary during the simulation times of interest. This typically worked out to be 1.5- to 3 times the plate/tape assembly thickness depending on desired simulation time. Elements were sized to capture small features in the shock wave structure. While elements as small as 2 microns were evaluated, we found that 10-micron mesh provided a good balance of convergence, structural detail, and computational turnaround time.

Materials

Aluminum 6061-O

The primary material of interest for this validation study is aluminum 6061-O. Quasi-static material properties were taken to be consistent with Polkinghorn and Lacy [13]. However, dynamic properties such as Equation of State (EOS) data and dynamic strength proved difficult to find. Dynamic applications typically employ the –T6 heat treatment condition of this alloy, and the fully annealed condition is under-represented in the literature. Split Hopkinson pressure bar data presented by Jenq and Sheu [14] were used as a starting point for a Johnson-Cook [15] plasticity model. The Johnson-Cook constitutive model is expressed as

$$\sigma_y = \left(A + B\varepsilon_p^n\right)\left(1 + C\ln\frac{\dot{\varepsilon}}{\dot{\varepsilon}_{ref}}\right)\left(1 - T^{*m}\right) \quad (1)$$

Where σ_y is the yield stress, ε_p is the effective plastic strain, $\dot{\varepsilon}\,p$ is the plastic strain rate, and $\dot{\varepsilon}\,ref$ is the reference plastic strain rate. *A*, *B*, and *n* are yield and strain-hardening parameters, *C* is a rate-hardening parameter, and *m* is a thermal softening parameter. The Johnson-Cook plasticity model is well-represented in the open literature, thus we do not discuss its details here. Parameters we employed are shown in Table 1. A comparison of the model to experimental data is shown in Fig. 5.

TABLE 1. Johnson-Cook Plasticity model parameters for wrought Aluminum 6061-0.

A	B	n	C	m	Poisson	Tmelt
55 MPa	210 MPa	0.475	0.07	1.0	.33	950. K

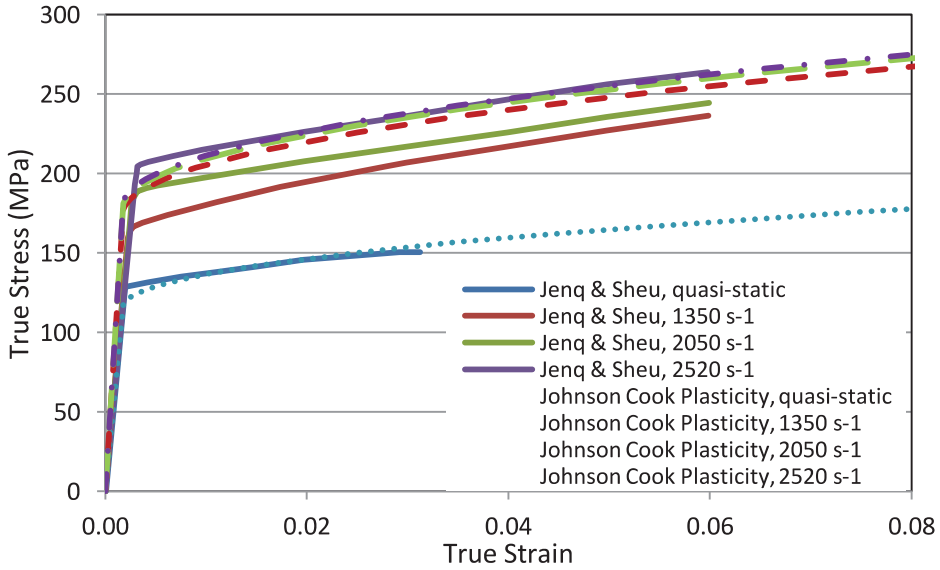

FIGURE 5. J-C plasticity model compared to Jenq and Sheu compressive data.

Polyurethane Cover Tape

We initially treated the clear polyurethane cover tape (3M 8547) solely as a hydrodynamic tamper. That is to say it has an equation of state to relate pressure, temperature, and density, but no tensile strength. However, our investigation led us to the conclusion that confinement strength of the cover has an important effect on the energy delivered to the aluminum plate: the upward-moving portion of the pressure wave that is reflected from the cover tape and back down into the aluminum as a positive pressure rather than as a relaxation wave depends in part on the tensile strength of the tape. While we have not yet settled on the most appropriate strength parameters for this product, we were able to employ the Sesame tabular equation of state data developed by Los Alamos and Sandia National Laboratories [16].

Polyvinyl Chloride (PVC) Absorption Tape

Black PVC absorption tape is also treated hydrodynamically. A simple Mie Gruneisen EOS model was developed from the shock compression data of Butler, Miller, and Bourne [17], and Carter and Marsh [18]. Specific heat data was taken from Dunlap [19]. It is important to note that PVC plastic is produced with varying amount of plasticizers. The tape we are using is highly plasticized and may not be optimally represented by the material employed in these experiments. This will be an area for refinement as we improve the model in the future. Figure 6 shows the model compared to the two sets of experimental U_s-u_p data.

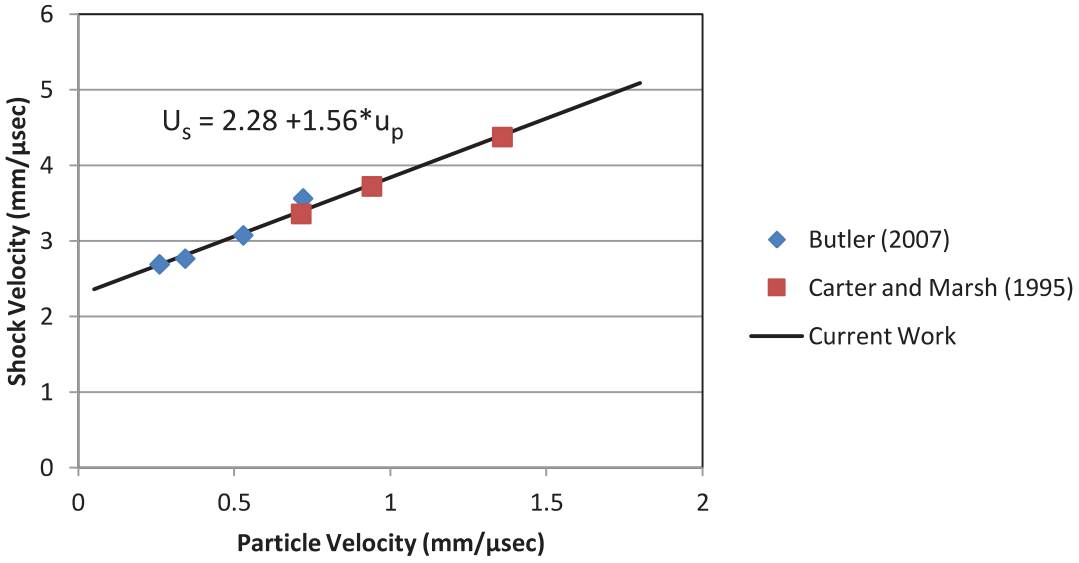

FIGURE 6. U_s-u_p relationship employed for PVC.

Dry Air

Domain volumes above and below the layered plate system were filled with dry air to avoid numerical difficulties associated with material/void interfaces. Air properties were incorporated from tabular EOS data (SESAME) in the software distribution. Its contribution to the computational results is negligible.

Energy Deposition

Simulations begin with deposition of energy into the black absorption tape. The nominal pulse duration has been measured experimentally by the manufacturer as 10 nanoseconds (10^{-8} sec). Spatially, the laser intensity is the typical Gaussian distribution of a single mode laser around the center of the spot. Because the excitation pulse is very short compared to the wave transit and pit formation times, the structural details of the input pulse do not overwhelmingly drive the response. However, it is important that the excitation energy be a smooth function both spatially and temporally. We have found that abrupt edges in either domain will cause secondary, unphysical shocks to form and propagate into the region of interest, distorting the response.

While several experiments are planned to further evaluate the effect of the spatial distribution of laser energy within the spot, we are currently employing a capped haversine radial distribution function as shown in Figure 7, with the cap (maximum intensity) to 60% of the nominal spot size, decaying smoothly through 25% intensity at the nominal spot radius, to zero at 120% of the nominal spot radius. This capped approach reduces the peak pressure in the tape material for a given total deposited energy, and smoothes the numerical response of the PVC tape material in that local region.

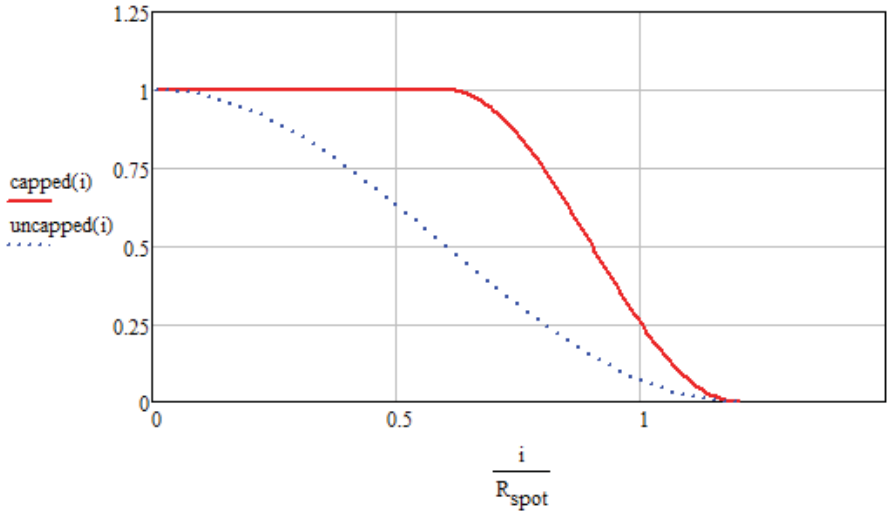

FIGURE 7. Example of a capped haversine radial energy distribution profile.

RESULTS

Comparison to Experiment

We consider 2 metrics to evaluate the accuracy of the simulations: the shape of the plate back surface velocity waveform, and the relationship between the peak back surface velocity and the depth of the front surface pit in the plate. Figure 8 shows the experimentally determined first pulse back surface wave form for a series of increasing laser energies as indicated by the flash lamp delay given in μs.

There are several important features to observe in Fig. 8. The "shoulder" on the leading edge of the wave traces indicates the elastic limit of the aluminum, and the fact that the limit increases with increasing shock intensity (particle velocity) indicates rate sensitivity. Correctly capturing these two features validates our parameters for initial yield strength and rate sensitivity in aluminum. The trailing edge shape is more complex, in that it is governed by the shape and duration of the positive pressure pulse applied to the front surface of the plate and the plastic work done in forming the surface pit. Increasing the confinement above the energy deposition zone and increasing plastic flow in the pit formation both tend to "fatten" the top of the back surface velocity trace.

Figures 9 and 10 compare the computed and experimentally determined velocity traces for low-energy and high-energy inputs, respectively. Studying the traces, it is apparent that while we are capturing the magnitude and leading-edge wave structure adequately, additional work is necessary to capture the complex interactions shaping the trailing edge of the velocity trace. Figure 11 gives us further guidance for improving simulation fidelity. This figure shows the relationship between back surface velocity (a measure of shock intensity) and the resultant surface pit depth. Here we see good agreement at lower energies diverging as shock energy increases. The agreement at lower energies supports the values selected for elastic and initial yield properties. The under-prediction of pit depth at high laser energies indicates that our parameters for post-yield flow are slightly too stiff. This directs our efforts toward refining the post-yield plastic flow response of the aluminum. This effort is ongoing.

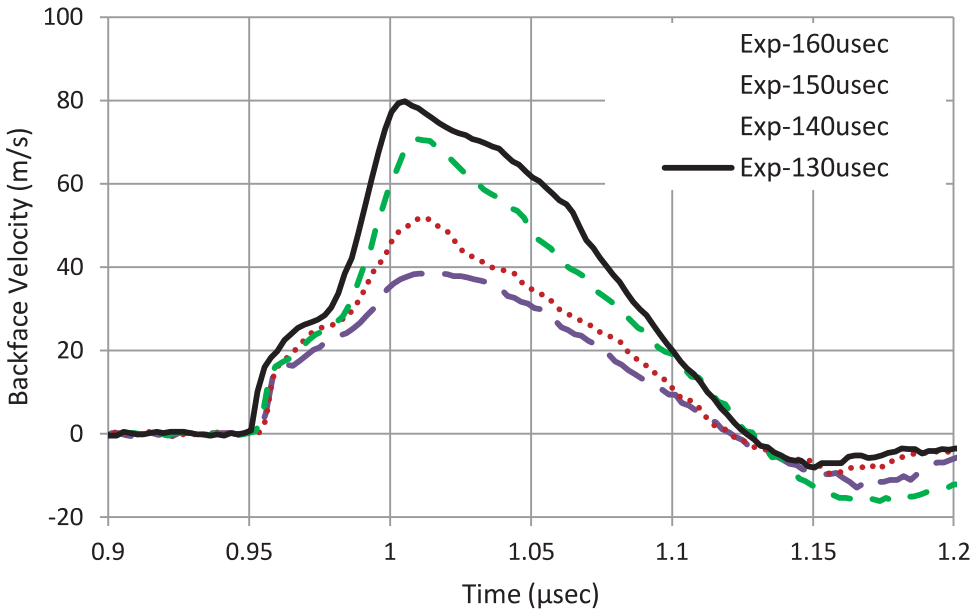

FIGURE 8. Experimentally determined back surface velocity traces.

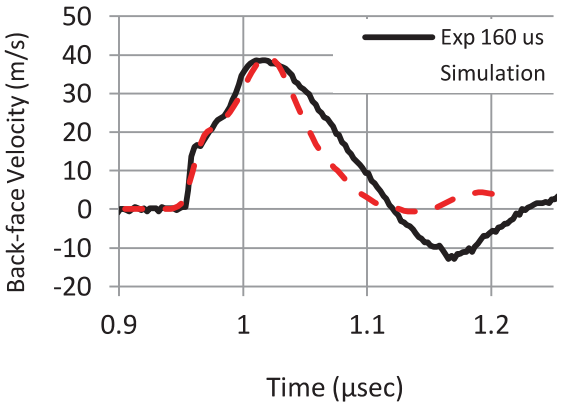

FIGURE 9. Comparison of simulation and experimental back surface velocities: low energy.

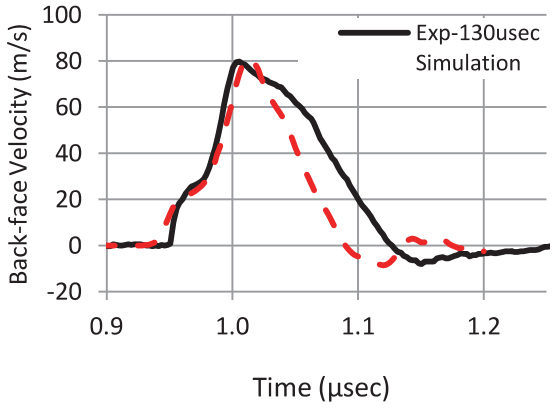

FIGURE 10. Comparison of simulation and experimental back surface velocities: high energy.

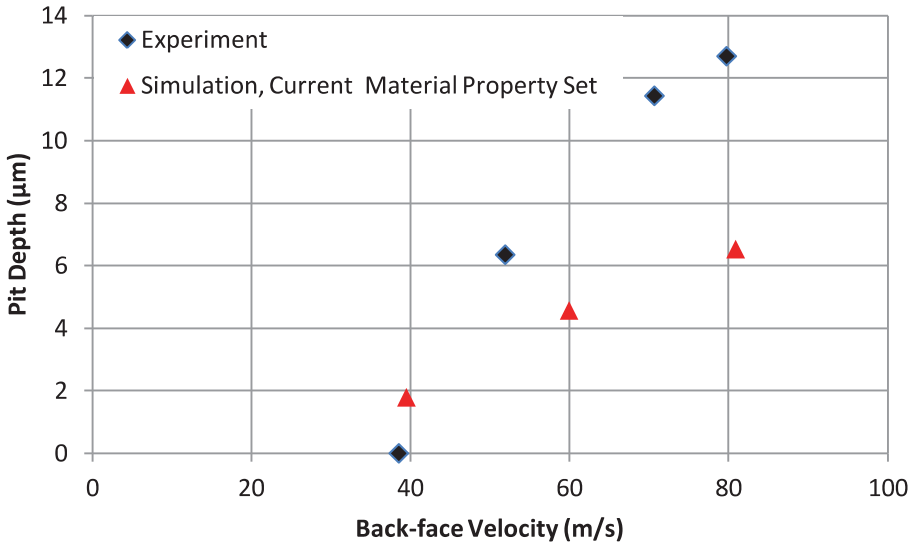

FIGURE 11. Pit depth vs. peak back surface velocity.

Future Work

Our focus for the near future is to refine the material parameters for wrought aluminum 6061-O that govern the post-yield hardening and flow, as well as investigating the extent to which confinement provided by the polyurethane cover tape affects the duration of the positive phase of the induced shock. Results too recent to be included herein are very promising on both fronts. With the model validated against experimental data, we anticipate expanding the method to calibrate and validate a loaded fuel plate model.

CONCLUSIONS

The ability to predict the intensity of internal stresses induced in layered fuel plate structures by the Laser Shock Technique is a necessary step in its adoption as a standard fuel characterization method. We are making good progress in developing an understanding of the parameters that influence the intensity and duration of the shock, and the plate materials' response to that shock. As it is developed, this understanding will be used to develop LST experiments fine-tuned for a variety of materials and layups. Comparisons between model predictions and experimental results will also allow verification of our understanding of those materials and will help to differentiate instances which only require summary testing from those requiring more rigorous testing.

REFERENCES

1. U. S. Department of Energy, "GTRI's Convert Program," http://nnsa.energy.gov/aboutus/ourprograms/dnn/gtri/convert, accessed August, 2014.
2. J. L. Vossen, "Measurements of film – substrate bond strength by laser spallation." *ASTM Spec. Tech. Publ. Am. Soc. Test. Mater.*, **640**: 122–133 (1978).
3. V. Gupta, et al, "Measurement of interface strength by laser-pulse-induced spallation," *Mater. Sci. Eng.* **A 126**, 105–117 (1990).
4. J. Yuan and V. Gupta, "Measurement of interface strength by the modified laser spallation technique: I. Experiment and simulation of the spallation process," *J. Appl. Phys.* **74**, 2388–2397 (1993).
5. V. Gupta and J. Yuan, "Measurement of interface strength by the modified laser spallation technique: II. Applications to metal/ceramic interfaces," *J. Appl. Phys*. **74** 2397– 2404 (1993).

6. J. Yuan, V. Gupta and A. Pronin, "Measurement of interface strength by the modified laser spallation technique: III. Experimental optimization of the stress pulse," *J. Appl. Phys*. **74**, 2405–2410 (1993).
7. C. Bolis, et al, "Physical Approach to Adhesion Testing Using Laser- Driven Shock Waves," *J. Phys. D: Appl. Phys*., **40(10)**, p 3155-3163 (2007).
8. M. Perton, A. Blouin and J.-P. Monchalin, "Adhesive bond testing of carbon–epoxy composites by laser shockwave", *J. Phys. D: Appl. Phys*., **44(3)**, 034012 (2011).
9. M. Arrigoni, et al., "Comparative study of three adhesion tests (EN 582 similar to ASTM C633 -LASAT (LASer Adhesion Test) - Bulge and blister test) performed on plasma sprayed copper deposited on aluminum 2017 substrates," *J. Adhes. Sci. Technol*., **20 (5)** pp. 471–487 (2006).
10. M. Perton, et al., "Laser shockwave technique for characterization of nuclear fuel plate interfaces", 39th Annual Review of Progress in QNDE, AIP Conf. Proc. 1511, 2013, 345-352.
11. M. Arrigoni, et al., "Laser Doppler Interferometer Based on a Solid Fabry- Perot Etalon for Measurement of Surface Velocity in Shock Experiments," *Meas. Sci. Technol*., **20(1)**, p 015302 (2009).
12. A. C. Robinson, et al., *ALEGRA User Manual*, Sandia National Laboratories, Report No. SAND-2014-1236, February 8, 2014.
13. S.T. Polkinghorne, J. M. Lacy. *Thermophysical and mechanical properties of ATR core materials*. EG&G Idaho Inc., Internal Technical Report, PG-T-91-031, August 1, 1991.
14. S. T. Jenq, and S. L. Sheu, "An Experimental and Numerical Analysis of High Strain Rate Compressional Behavior of 6061-0 Aluminum alloy," *Computers and Structures*, **52(1)**, pp 27-34 (1994).
15. G. R. Johnson, and W. H Cook, "A constitutive model and data for metals subjected to large strains, high strain rates and high temperatures," *Proc. 7th International Symposium on Ballistics*, pp. 541–547 (1983).
16. G. I. Kerley and T. L. Christian-Frear, *Sandia Equation of State Data Base: seslan File*, Sandia National Laboratories report SAND93-1206 (1993).
17. S. Butler, J. C. F. Millett, and N. K. Bourne, "Shock Induced Equation of State of Polyvinylchloride," *Shock Compression of Compressed Matter – 2007*, American Institute of Physics, 2007.
18. W. J. Carter, and S. P. Marsh, *Hugoniot Equation of State of Polymers*, LA-13006-MS, Los Alamos National Laboratory, 1995.
19. Dunlap, L. H., "Specific Heats of Poly (vinyl Chloride) Compositions," *J. Polymer Sci, Part A-2*, **4**, 673-684 (1966).